Dyes and Pigments 86 (2010) 227–232

Contents lists available at ScienceDirect

Dyes and Pigments

journal homepage: www.elsevier.com/locate/dyepig

The in situ characterization of bacteriochlorophyll *c* in Langmuir monolayers using polarized UV–vis spectroscopy☆

Alina Dudkowiak [a,*], Michał Czapski [a], Michał Kotkowiak [a], Jun Miyake [b]

[a] Institute of Physics, Faculty of Technical Physics, Poznan University of Technology, Nieszawska 13a, 60-965 Poznan, Poland
[b] Center for Nanobio Integration, The University of Tokyo, 7-3-1 Hongo, Tokyo 113-0033, Japan

ARTICLE INFO

Article history:
Received 29 October 2009
Received in revised form
15 January 2010
Accepted 19 January 2010
Available online 28 January 2010

Keywords:
Bacteriochlorophyll *c*
Extinction coefficient
Hansen's optical theory
Langmuir monolayer
Molecular orientation
Refraction index

ABSTRACT

The in situ arrangement of bacteriochlorophyll *c* in a Langmuir monolayer was characterized. Hansen's optical theory was applied to the three-layer system, air/pigment monolayer/water and the correlation between surface pressure and the orientation angle of the bacteriochlorophyll transition dipole moments was deduced. On the basis of the *s*- and *p*-polarized UV–vis reflection–absorption and transmission spectra, respectively, the refraction index and extinction coefficient of the red (Q_y) band of both the monomeric and aggregated forms of the pigment were estimated.

1. Introduction

Bacteriochlorophyll (BChl) *c* is one of the photosynthetic pigments and a key ingredient in light-harvesting antennas (chlorosomes) of green sulfur bacteria [1]. The BChl *c* molecules are known for their ability to form the rod-shaped self-assembly structures characterized by high efficiency of energy transfer. Understanding the architecture of the chlorosomes, in the absence of structural evidence from crystallographic methods, is still difficult and controversially discussed in literature [2–6].

The molecular orientation is an important factor for many biological functions of pigments in the photosynthetic systems. The Langmuir monolayer approach is a unique technique applied to mimic two-dimensional biological systems but it is also a powerful method to control the interaction of molecules depending on their mutual distance, orientation and packing in ultrathin film used in molecular devices and sensors. Pigment molecules in Langmuir monolayers can be easily arranged in a defined way. This property seems to be crucial for the supramolecular electronics, where the manipulation of single dye molecules can help design electronic systems with submolecular precision. Hence, studies of pigment Langmuir monolayers can help investigate and explain important properties of molecular organization of in vivo light-harvesting systems. Moreover, the pigment molecules can also be considered as an important material for environment-friendly molecular engineering, especially for applications in bioinspired nanodevices as hybrid solar cells [7] operated under low-light illumination condition, four-step molecular switch [8] or molecular (semi) conductive wires [9].

In recent years, the arrangement of BChl *c* molecules in mono- and multilayers on highly ordered pyrolytic graphite (HOPG), molybdenum disulfide (MoS_2), quartz plate or water subphase has been characterized by different experimental methods including scanning tunneling microscopy (STM) [10–12], solid-state nuclear magnetic resonance (NMR) [13], cryoelectron microscopy [14], Fourier-transform infrared (FT-IR) and UV–vis absorption spectroscopy [15], Brewster angle microscopy (BAM) [16] as well as surface pressure-area (π-*A*) isotherm [17,18]. It was found that in layers, the pigment molecules could exist in different forms such as monomers, dimers, tetramers, oligomers and/or polymers, depending on the conditions and preparation methods [10–12,15–18]. It is known [19] that the isotherms of Langmuir monolayer are sensitive to the character of interactions between pigment monomers on the water subphase. This fact has prompted

☆ Dedicated to Professor Danuta Frąckowiak on the occasion of her eighty-fifth birthday.

* Corresponding author. Tel.: +48 61 665 3181; fax: +48 61 665 3178.
E-mail address: alina.dudkowiak@put.poznan.pl (A. Dudkowiak).

0143-7208/$ – see front matter © 2010 Elsevier Ltd. All rights reserved.
doi:10.1016/j.dyepig.2010.01.007

us to analyze and estimate the molecular orientation in monolayers by independent methods. For monolayers at the air–water interface the reflection–absorption methods in the infrared [19] and UV–vis [20] spectroscopic regions can be used. In this study, the polarized visible (UV–vis) reflection–absorption spectra of the pigment were measured in situ at different surface pressures. Applying the Hansen's optical theory to interpret the experimental results, a quantitative analysis of BChl *c* organization in a Langmuir monolayer was made. A similar analysis for the photosynthetic pigment of chlorophyll (Chl) *a* was made elsewhere [20]. Using the *s*- and *p*-polarized reflection–absorption spectra, the refractive index and extinction coefficient for monomeric and aggregated forms of BChl *c* in a monolayer were for the first time estimated. The molecular arrangement of BChl *c* at the air–water interface was discussed taking into regard the relation between the surface pressure and the orientation angle of the BChl *c* species and the models proposed in literature [14,21].

2. Materials and methods

BChl *c* was isolated from the sulfur bacteria *Prosthecochloris aestuarii*; extraction, purification and identification procedures were described earlier [22]. The pigment used was a mixture of spectrally indiscernible homologs differing in the degree of alkylation on the chlorin ring at positions 8 and 12 (R_8 and R_{12}, respectively) (Fig. 1A).

The measurements of the (π-A) isotherm were carried out by use of KSV-5000 Langumir trough operated in conjunction with a Wilhelmy balance ($\pm$0.04mN m^{-1}). The pigment from the stock chloroform solution (0.1mM) was spread on the subphase (2mM Tris/HCl, 2mM $CaCl_2$, 0.5mM sodium ascorbate, pH 8.2) buffer system. The solvent used to dissolve the pigment was allowed to evaporate for 15min after spreading. The resistivity of purified water used for experiments was $1.82 \cdot 10^6\Omega$m. The rate of the teflon barriers compression was set to be 3mm min^{-1}. All experiments were performed in dim light, with minimal difference between the air and the subphase temperatures (20$\pm$1)°C to prevent a capillary convection effect in the subphase.

In situ polarized visible (UV–vis) reflection–absorption spectra of BChl *c* Langmuir monolayer were measured on a MCPD-1000 (Otsuka Electronics) spectrophotometer equipped with optical fiber probes and photodiode array detector [20]. The experiments were performed for both *p*- and *s*-polarized beams of the light electric vector parallel and perpendicular (normal) to the plane of incidence, respectively (Fig. 2). The angle of incidence (θ_1) was at 37.5° to the water surface normal. The reflected beam was collected by the second fiber and transmitted to the detector.

The polarized transmission spectra of the BChl *c* Langmuir–Blodgett (LB) films deposited onto quartz plates were recorded by a Cary 4000 (Varian) spectrophotometer equipped with a Glan–Thompson polarizer and an angular sample holder. The measurements were performed with the light electric vector parallel and perpendicular to the direction of the emerging LB layer, respectively.

All quantitative calculations were performed with the program *Mathematica* version 5.0.

3. Results and discussion

The π-A isotherm of the BChl *c* Langmuir monolayer and the compression modulus (1/C), calculated from the formula (1/C)=$-A$ (dπ/dA), are shown in Fig. 3. The surface pressure begins to increase at the surface area of about 2.67nm^2 molecule^{-1}. After passing the liquid-expanded region, the isotherm exhibits an inflection point and the compression modulus values decrease sharply, suggesting

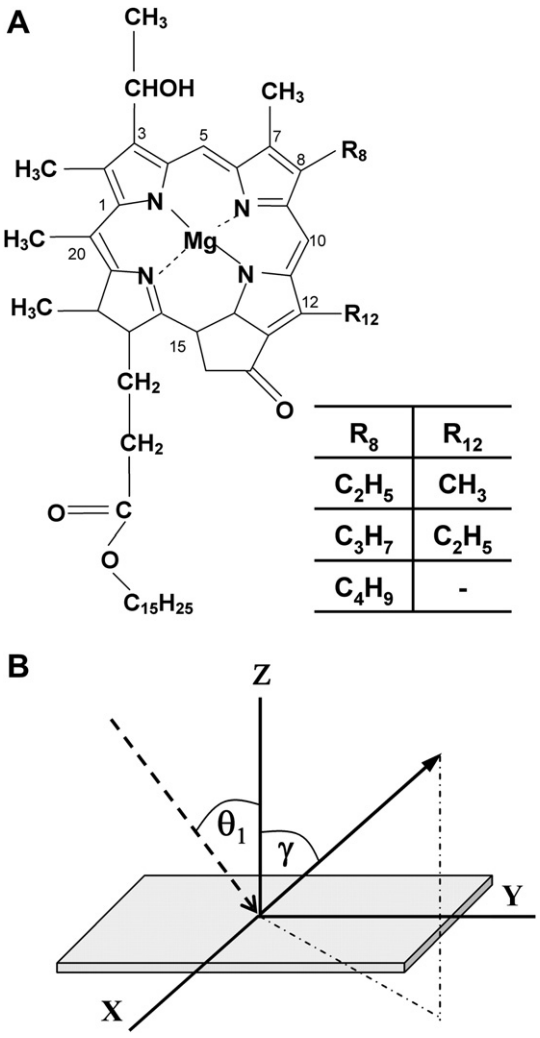

Fig. 1. (A) Molecular structure of BChl *c* and its homologs; and (B) the coordinate frame (*X*, *Y*, *Z*) of the pigment molecules in Langmuir monolayer; *Z*-axis – the surface normal, γ – orientation angle, θ_1 – incidence angle.

a phase change. Above 13.5mN m^{-1}, the isotherm slope decreases and the linear part begins seems to be the collapsed film region, but the surface pressure continues to increase up to 24mN m^{-1}. By extrapolation of the linear part of the isotherm, the limiting molecular area is obtained to be 2.43nm^2 molecule^{-1} which is extraordinarily large for the BChl *c* molecule.

It was shown earlier that BChl *c* exists at least in two different forms at the water interface [16]. Up to about 13mN m^{-1}, the monomeric form is dominant and above the inflection point a new Q_y band (around 730nm) appears in the absorption spectrum indicating the formation of aggregated species. To explore the molecular aggregation properties of BChl *c*, in our previous study the BAM technique [16] was used. Inhomogeneous topologies were found in the pigment monolayer, in the beginning the domains organized in islands at 0mN m^{-1} and finally a uniform film covered the water surface. When in the gaseous phase, the molecules were spontaneously aggregated to form molecular domains and were apart from each other on the water surface, which means that the monomeric compound underwent strong molecular interactions [19]. In such a case the film structure is formed in each domain at the very initial stage after the spread of the monomer molecules on the subphase, and the isotherm would largely be different from that of the weak-interacting molecules not only in the shape but also in

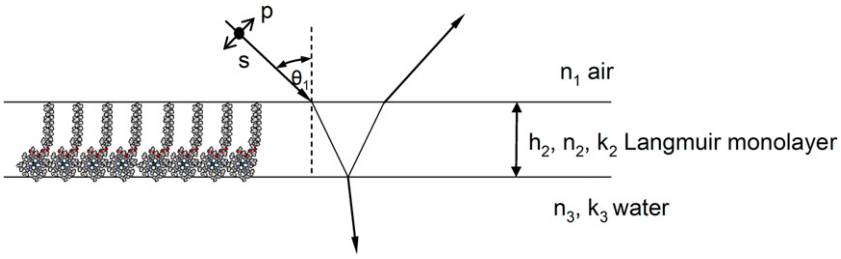

Fig. 2. A three-layer system of air/pigment Langmuir monolayer/water.

the limiting molecular area. Therefore, study of Langmuir monolayers can provide information on the degree of molecular interactions. On the basis of the 1/C-A dependence it seems that the phase change, observed to take place on contraction of the area occupied by the molecule is a consequence of the dye molecules reorientation on the subphase and breaking of the coordination bonds between the dye and water molecules.

Because for the strongly interacting molecules such as BChl *c*, it is impossible to draw conclusions on the molecular arrangement by studying the π-*A* isotherm, hence it was reasonable to employ the polarized visible reflection–absorption spectroscopy to get some information on the in situ molecular orientation of BChl *c* pigment molecules on the water interface.

Exemplary polarized reflection–absorption spectra are shown in Fig. 4A. The arrows (Fig. 3) indicate the surface pressure (or areas) at which the reflection–absorption spectra were taken. The reflection–absorbance is measured as $\log(R_0/R)$ where R_0 and R are the reflectivity of the pure subphase and that of the subphase covered with the monolayer, respectively. A slight difference in the reflection–absorption spectra recorded for *s*- and *p*-polarized light was observed and the higher absolute values were obtained for the latter, irrespectively of the pigment species (Fig. 4). There are two characteristic bands in different spectral regions: the Soret band in the blue-violet region with the peak at about 426nm and a shoulder at 450nm, as well as the red bands with peaks at 671 and 734nm. The Soret (*B*) band related to the ($S_0 \rightarrow S_2$) transitions and the red (*Q*) band assigned to the ($S_0 \rightarrow S_1$) transitions give rise to the observed B_x, B_y, and Q_x, Q_y bands, respectively.

The Q_y band of the polarized reflection–absorption spectra (from Fig. 4A) could be satisfactorily deconvoluted into three Gaussian components (not shown). Table 1 presents results of the Gaussian analysis. Each polarized spectrum was deconvoluted using the same bandwidth of the corresponding Gaussian component. According to literature [23–25] the 671nm band could be assigned to a monomer and/or a high-energy transition of tetramer of BChl *c*, whereas the red-shifted 734nm broad absorption band includes the contributions from 719 and 742nm bands, which can belong to BChl *c* J-type aggregate forms, i.e. a low-energy singlet level of tetramer and oligomer, respectively. As follows from Table 1, the percent contribution of particular species of the pigment in the *s*- and *p*-components of reflection–absorption spectra observed is almost the same with the calculation accuracy. However, the integral absorption for all BChl *c* forms are twice greater in *p*- than

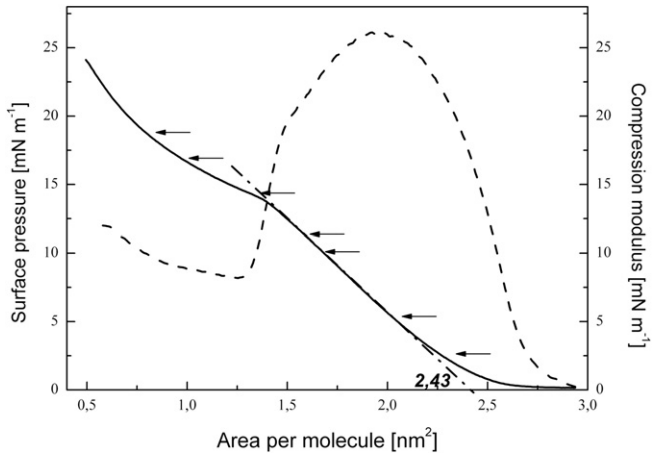

Fig. 3. The surface pressure-area isotherm and the compression modulus of BChl *c* Langmuir monolayer (arrows indicate points at which the reflection–absorption spectra were collected).

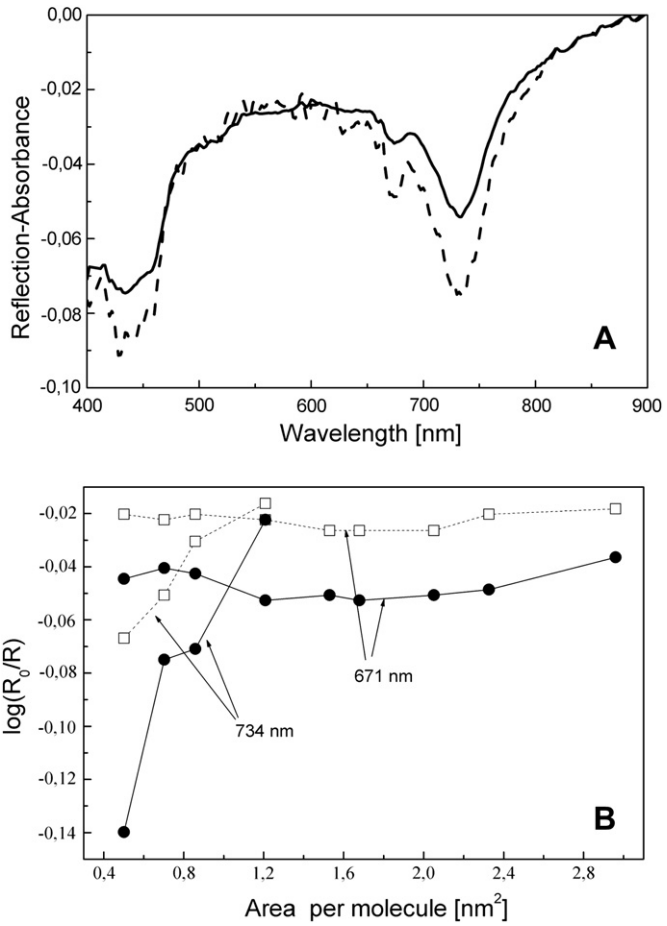

Fig. 4. (A) Polarized reflection–absorption spectra of BChl *c* monolayer observed at π=20mN m^{-1}; *s*- and *p*-polarizations (solid and dashed line, respectively); and (B) the reflection–absorbance of Q_y BChl *c* bands as a function of the layer compression for *s*-(□) and *p*- (●) polarizations.

Table 1
Gaussian analysis of the reflection–absorption spectra of BChl *c* in the Langmuir monolayer (from Fig. 4A); λ – maximum position, FWHM – full-width at half maximum, A – integral absorption.

Polarization	λ (nm)/(cm^{-1})	FWHM (cm^{-1})	Area (%)	A (a.u.)
s	742/13469	700	28.4	12.4
	719/13894	1064	57.5	25.1
	671/14883	456	14.0	6.1
p	742/13469	700	26.3	20.4
	719/13894	1064	56.9	44.1
	671/14883	456	16.8	13.0

in *s*-polarized components and tetramers are the preferred type of aggregation species in the Langmuir monolayer.

Fig. 4B shows a correlation between the reflection–absorbance intensity of Q_y BChl *c* band and the layer compression. The values of the reflection–absorption of the monomeric form slightly vary with increasing surface pressure, whereas for the aggregated form they sharply drop with decreasing area per molecule. Analysis of the absolute values of the reflection–absorbance of the aggregated band shows that it increases rapidly for *p*- and *s*-polarization with increasing layer compression.

Applying the optical theory proposed by Hansen [26] it was possible to perform quantitative evaluation of molecular orientation in BChl *c* Langmuir monolayer. This theory is based on modified Fresnel equations for multi-phase systems for which the behaviour of electromagnetic wave can be predicted. A particular case is the three-phase plane-bound system described by Hansen's optics [26]. This three-phase system consists of two semi-infinite layers 1 and 3 separated by the finite layer 2. In the system studied layers 1, 2 and 3 are the air, BChl *c* Langmuir monolayer and water subphase, respectively (Fig. 2). Because of the similarity in the molecular structure of Chl *a* and BChl *c* it was assumed that the thickness of the pigment layer (h_2) was 2.13nm [27]. At these assumptions it is possible to calculate the reflection–absorbance values for both *s*- and *p*-polarized beams (A_{sy} and A_{px}, A_{pz}, respectively) [28,29] using Eqs. (1–3):

$$A_{sy} = -\frac{16\pi}{\ln 10}\left(\frac{\cos^2\theta_1}{n_3^2-1}\right)n_2h_2k_{2y}\nu_0 \tag{1}$$

$$A_{px} = \frac{16\pi}{\ln 10}\left(\frac{\cos\theta_1\left(n_3^2-n_1\sin^2\theta_1\right)}{n_3^2-n_1\sin^2\theta_1-n_3^4\cos^2\theta_1}\right)n_2h_2k_{2x}\nu_0 \tag{2}$$

$$A_{pz} = -\frac{16\pi}{\ln 10}\left(\frac{\cos\theta_1}{\frac{n_3^2-n_1^2\sin^2\theta_1}{n_3^4}-\cos^2\theta_1}\right)\frac{\sin^2\theta_1}{\left(n_2^2+k_{2z}^2\right)^2}n_2h_2k_{2z}\nu_0 \tag{3}$$

where θ_1 is the angle of incidence and n_1, n_2, n_3 are refractive indices for air, pigment layer, water, respectively; k_{2i} and α_{2i} ($=4\pi k_{2i}\nu_0$) are *i*-th components of extinction and absorption coefficients of BChl *c* (for $i=x, y, z$); ν_0 is the wavenumber of the maximum for the reflection–absorption pigment band.

The orientation of BChl *c* in the monolayer was estimated for the monomeric and aggregated forms to which the Q_y bands at 671 and 734nm, respectively were assigned. The Soret band has a complex nature and a rough shape, which makes it difficult to carry out accurate calculation. The searched values of n_2 and k_{2i} could be determined as described below.

Using Hansen's equations [26] for the system investigated, it was possible to evaluate the refractive index for pigmented Langmuir monolayer by fitting the calculated values from Eqs. (4) and (5) to experimentally obtained values of reflectivity (R) for both *s*- and *p*-polarization:

$$R_s = \left|\frac{(m_{11}+m_{12}n_3\cos\theta_3)n_1\cos\theta_1-(m_{21}+m_{22}n_3\cos\theta_3)}{(m_{11}+m_{12}n_3\cos\theta_3)n_1\cos\theta_1+(m_{21}+m_{22}n_3\cos\theta_3)}\right|^2, \tag{4}$$

$$R_p = \left|\frac{\left(m_{11}+\frac{m_{12}\cos\theta_3}{n_3}\right)\frac{\cos\theta_1}{n_1}-\left(m_{21}+\frac{m_{22}\cos\theta_3}{n_3}\right)}{\left(m_{11}+m_{12}\frac{\cos\theta_3}{n_3}\right)\frac{\cos\theta_1}{n_1}+\left(m_{21}+m_{22}\frac{\cos\theta_3}{n_3}\right)}\right|^2, \tag{5}$$

and m_{vw} are the elements of the M_2^s and M_2^p characteristic matrices (6, 7) for *s*- and *p*-polarization with

$$M_j^s = \begin{bmatrix} \cos(2\pi\nu h_j n_j\cos\theta_j) & \frac{-i}{n_j\cos\theta_j}\sin(2\pi\nu h_j n_j\cos\theta_j) \\ -in_j\cos\theta_j\sin(2\pi\nu h_j n_j\cos\theta_j) & \cos(2\pi\nu h_j n_j\cos\theta_j) \end{bmatrix}, \tag{6}$$

$$M_j^P = \begin{bmatrix} \cos(2\pi\nu h_j n_j\cos\theta_j) & \frac{-in_j}{\cos\theta_j}\sin(2\pi\nu h_j n_j\cos\theta_j) \\ \frac{-i\cos\theta_j}{n_j}\sin(2\pi\nu h_j n_j\cos\theta_j) & \cos(2\pi\nu h_j n_j\cos\theta_j) \end{bmatrix}, \tag{7}$$

where θ_j, n_j and h_j are the angle of incidence (or refraction), the refractive index and the thickness of *j*-th layer, ν – the wavenumber of incidence light.

The obtained values of refractive indices are substantially the same, i.e. n_{2s}=1.17664 and 1.17664 (for *s*-polarization) and n_{2p}=1.17663 and 1.17662 (for *p*-polarization) for the monomer and aggregate species, respectively.

The *s*- and *p*-polarized transmission spectra of BChl *c* LB films on quartz (not shown) were almost equal and no anisotropy was observed. Because of the lack of dichroism in the transmission spectra, the isotropic k_2 value is related to k_{2i} ($i=x, y$ and z) values by the equation $3k_2=k_{2x}+k_{2y}+k_{2z}$ for the perfect parallel ($k_{2x}=k_{2y}$, $k_{2z}=0$) and normal orientation ($k_{2x}=k_{2y}$) of the pigment transition moment. The calculated isotropic extinction coefficients (k_2) are 1.38 and 1.42 at 671 and 734nm, respectively.

From the relation between the area per molecule (or surface pressure) and the arrangement of the BChl *c* in the Langmuir layer, described by the orientation angle (γ) against the surface normal for a transition dipole moment (Fig. 1B), can be estimated. For flat-shaped chlorophyll molecules the dipole transition moments are oriented parallel to the porphyrin ring, therefore the orientation angle (γ) calculated from both *p*- and *s*-polarized reflection–absorbances can be used to draw conclusions about the pigment porphyrin ring orientation. The observed A_s and A_p values of the reflection–absorbance of Q_y pigment bands are determined by the γ angle using Eqs. (8) and (9):

$$A_s = A_{sy}\sin^2\gamma \tag{8}$$

$$A_p = A_{px}\sin^2\gamma + A_{pz}\cos^2\gamma \tag{9}$$

The theoretically obtained reflection–absorbance values for *s*- and *p*-polarization components are negative irrespective of the orientation angle and they decrease with increasing angle value. These results are compared to the experimental values to determine the average orientation angle of the pigment transition moments in the monolayer as a function of the layer compression (Fig. 5). A slight decrease in the orientation angle in the range

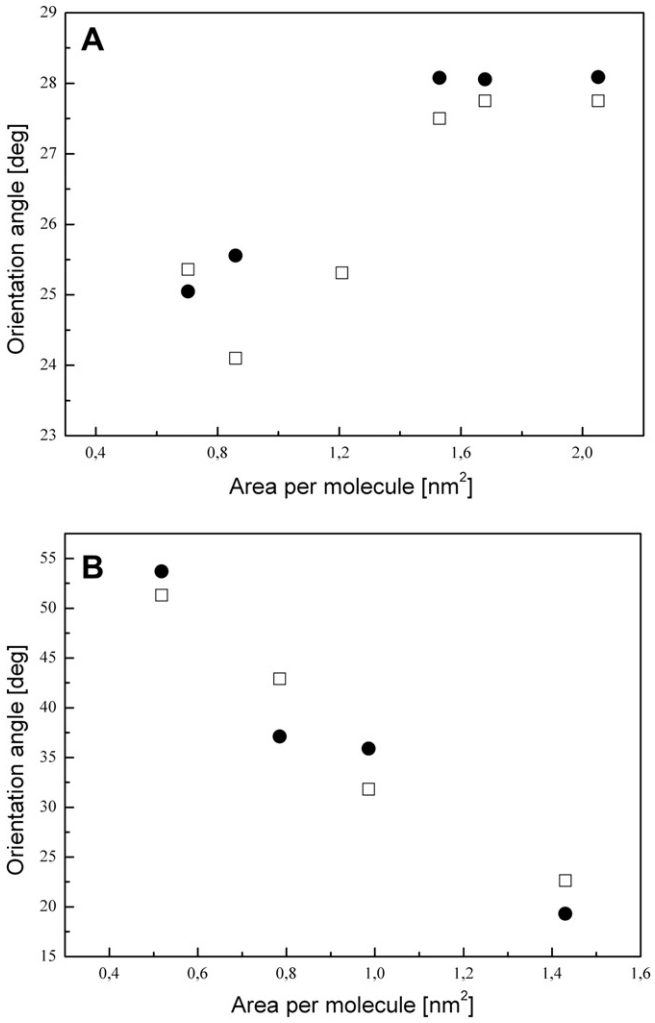

Fig. 5. Changes in the orientation angle of the BChl *c* transition moments with monolayer compression for *s*- and *p*-polarization observed for: (A) monomer; and (B) aggregates; *s* (□) and *p* (●) polarizations.

(28°–24°) as a function of the area per molecule is observed for the BChl monomers (Fig. 5A). At the distance and orientation of BChl *c* rings (γ=26°) favorable for the pigment–pigment interactions, the self-assembled aggregates are formed which is manifested in the 1/C-A dependence as a phase change. For the aggregates the tilt angle increase from 21° (at inflection point) to 52° (with monolayer compression up to 20mN m^{-1}) (Fig. 5B) was obtained. The calculated γ angles are similar for the *s*- and *p*-polarized light within the experimental error. The average orientation angle of the transition dipole moments to the surface normal in Langmuir layer calculated for BChl *c* aggregates is almost equal to magic angle, which could suggest that the refractive indices in all directions are equal and/or homogeneous distribution of dipole transitions is possible. But it is necessary to consider that the tilt of the γ angle reflect the situation of transition moments of at least two forms.

Strong mutual interactions between the bacteriochlorophyll molecules practically prevents drawing conclusions on the mechanism of the aggregation process and orientation of the dye molecules on the basis of the π-*A* isotherm, while the results obtained from the polarized reflection–absorption spectra permit suggesting a possible arrangement of the BChl *c* molecules in monolayers. With increasing Langmuir layer compression, the porphyrin planes of individual dye molecules begin to rise up from the subphase, which suggests decreasing values of the orientation angle (γ). Near the inflection point the molecular orientation of the pigment seems to be suitable to form BChl *c* aggregates, which leads to a decrease in the layer compressibility. It seems that in the Langmuir layer the non-aggregated single molecules (monomers) occupy greater area than the molecules in aggregates (e.g. tetramers, oligomers) formed by the pigment–pigment mutual interaction. So the compression of the pigment layer results in the aggregate formation and also in decreasing mean orientation angle. The transformation from monomer to large aggregate species is continuous and the calculated orientation angle allows also concluding about a possible mechanism of aggregation in the compressed BChl *c* Langmuir monolayers. It is known [1,15,30,31] that the self-aggregation driving force is the Mg…O–H…O=C(13^1) interaction which leads to formation of a giant hollow cylinder similar to the BChl *c* rods in the chlorosome. On the basis of the interactions a lot of models for small and large aggregates have been proposed depending on the homolog species, solvent interaction, model system, etc. [23,30–32]. It was suggested [23,32] that small and large aggregate formations have different bonding requirements. Our experimental results and theoretical predictions provide interesting insight into the aggregation process and prove that small and large aggregates can be formed by a continuous process. The process is initiated not only by a simple decrease in the area occupied by the molecules but it is clear that first of all a special molecular orientation of the BChl *c* rings is required.

A similar molecular organization of self-assembling chlorosomal pigments has been reported by others [14,21]. In ref. [21] zinc chlorin has been found to form highly ordered double-stacked π-aggregates on HOPG. The planes of chlorin molecules were tilted with respect to the surface at the angle of 35° (i.e. at the angle of 55° against the surface normal similarly as in the Langmuir monolayer). To explore the chlorosome architecture, two supramolecular arrangements with *syn-anti* BChl *c* monomer stacks running parallel or perpendicular to the tube axis, producing similar O–H…O=C(13^1) exciton delocalization pathways have been proposed [14]. The inclination of the optical transition dipole moment of pigment with respect to the long axis of the tube in proposed structures was found also around 55°. It confirms that the two-dimensional system formed at the water interface mimics to some extent the in vivo chlorosome-like structure and can be treated as the supramolecular complexes to study the function of photosynthetic antennae systems. The knowledge of the pigment molecular orientation as a function of surface pressure obtained from the reflection–absorption spectra is important to find the deposition conditions at which the thin layer maintaining the desired pigment orientation on a solid surface can be manufactured.

In conclusion, the experimental results on the orientation of the BChl *c* molecules in the Langmuir monolayer were combined with theoretical calculations obtained on the basis of the Hansen theory. The refractive index and extinction coefficient for the monomeric and aggregated forms of BChl *c* in the monolayer were evaluated. Quantitative analysis of BChl *c* orientation showed that the porphyrin ring of pigment monomers rise up from water with Langmuir monolayer compression till the distance and orientation of BChl *c* rings are favorable for the pigment–pigment interaction. The tentative step-by-step aggregation process of BChl *c* molecules in the two-dimensional network covering the subphase surface begins with monomers followed probably by tetramer formation and continues with transformation to oligomers. The formation of dimers as intermediate species is not observed in the in situ measured spectra. The orientation of the single monomer molecules is different from that of the aggregate structures in the monolayer, for which the mean orientation angle increases up to 52° with increasing layer compression.

Acknowledgments

This work was supported in part by the Polish Ministry of Sciences and Higher Education (2008–2011) and Poznan University of Technology.

References

[1] Olson JM. Chlorophyll organization and function in green photosynthetic bacteria. Photochem Photobiol 1998;67:61–75.
[2] Nozawa T, Ohtomo K, Suzuki M, Nakagawa H, Shikama Y, Konami H, et al. Structures of chlorosomes and aggregated BChl *c* in *Chlorobium tepidum* from solid state high resolution CP/MAS ^{13}C NMR. Photosynth Res 1994;41:211–23.
[3] Balaban TS, Holzwarth AR, Schaffner K, Boender G-J, de Groot HJM. CP-MAS ^{13}C-NMR dipolar correlation spectroscopy of ^{13}C-enriched chlorosomes and isolated bacteriochlorophyll-*c* aggregates of *Chlorobium tepidum*: the self-organization of pigments is the main structural feature of chlorosomes. Biochemistry 1995;34:15259–66.
[4] van Rossum B-J, Steensgaard DB, Mulder FM, Boender GJ, Schaffner K, Holzwarth AR, et al. A refined model of the chlorosomal antennae of the green bacterium *Chlorobium tepidum* from proton chemical shift constraints obtained with high-field 2D and 3D MAS NMR dipolar correlation spectroscopy. Biochemistry 2001;40:1587–95.
[5] Psencik J, Ma Y-Z, Arellano JB, Hala J, Gillbro T. Internal structure of chlorosomes from brown-colored *Chlorobium* species and the role of carotenoids in their assembly. Biophys J 2004;87:1165–72.
[6] Jochum T, Reddy ChM, Eichhőfer A, Buth G, Szmytkowski J, Kalt H, et al. The supramolecular organization of self-assembling chlorosomal bacteriochlorophyll *c*, *d*, or *e* mimics. Proc Natl Acad Sci USA 2008;105:12736–41.
[7] Linke-Schaetzel M, Bhise AD, Gliemann H, Koch T, Schimmel T, Balaban TS. Self-assembled chromophores for hybrid solar cells. Thin Solid Films 2004; 451-452:16–21.
[8] Iancu V, Hla S-W. Realization of a four-step molecular switch in scanning tunneling microscope manipulation of a single chlorophyll-*a* molecules. Proc Natl Acad Sci USA 2006;103:13718–21.
[9] Schenning APHJ, Meijer EW. Supramolecular electronics: nanowires from self-assembled π-conjugated systems. Chem Commun 2005;26:3245–58.
[10] Jiang Y, Xu Q, Wan L, Wang C, Fang X, Bai C, et al. Direct observation of monomer film structure of bacteriochlorophyll *c*. Chinese Sci Bull 2003;48: 2307–10.
[11] Mőltgen H, Kleinermanns K, Jesorka A, Schaffner K, Holzwarth AR. Self-assembly of [Et,Et]-bacteriochlorophyll c_F on highly oriented pyrolytic graphite revealed by scanning tunneling microscopy. Photochem Photobiol 2002;75:619–26.
[12] Xu Q-M, Wan L-J, Yin S-X, Wang Ch, Bai Ch-L, Ishii T, et al. A dimeric structure of bacteriochlorophyllide *c* molecules studied by scanning tunnelling microscopy. J Phys Chem B 2002;106:3037–40.
[13] Egawa A, Fujiwara T, Mizoguchi T, Kakitani Y, Koyama Y, Akutsu H. Structure of the light-harvesting bacterichlorophyll *c* assembly in the chlorosomes from *Chlorobium limicola* determined by solid-state NMR. Proc Natl Acad Sci USA 2007;104:790–5.
[14] Ganapathy S, Oostergetel GT, Wawrzyniak PK, Reus M, Chew AGM, Buda F, et al. Alternating *syn-anti* bacteriochlorophylls from concentric helical nanotubes in chlorosomes. Proc Natl Acad Sci USA 2009;106:8525–30.
[15] Uehara K, Tachibana T, Tsunooka M, Ozaki Y. Interconversion of bacteriochlorophyll *c* aggregates in solid films upon organic vapor treatment. Photochem Photobiol 1995;62:496–501.
[16] Dudkowiak A, Kusumi T, Nakamura C, Miyake J. Spectroscopic properties of bacteriochlorophyll *c* in Langmuir monolayers in the absence and presence of amphiphilic peptides. J Photochem Photobiol A 2000;134:177–83.
[17] Dudkowiak A, Biadasz A, Bartczak A. Spectral and thermodynamic characterization of bacteriochlorophyll *c* and dipalmitoylphosphatidylcholine in the binary mixed monolayers. J Mol Struct 2008;887:128–34.
[18] Dudkowiak A, Bartczak A. Analysis of molecular organization of BChl *c* and its Mg-free derivative in Langmuir monolayers. Sci Bull Phys 2006;26:7–12.
[19] Hasegawa T, Sato Y, Kakuda H, Li Ch, Orbulescu J, Leblanc RM. Study of molecular aggregation of artificial amyloid in Langmuir monolayer by infrared spectroscopy. J Phys Chem B 2008;112:1391–6.
[20] Okamura E, Hasegawa T, Umemura J. Quantitative analysis of molecular orientation in chlorophyll *a* Langmuir monolayer: a polarized visible reflection spectroscopic study. Biophys J 1995;69:1142–7.
[21] Huber V, Lysetska M, Wűrthner F. Self-assembled single- and double stack π-aggregates of chlorophyll derivatives on highly ordered pyrolytic graphite. Small 2007;3:1007–14.
[22] Swarthoff T, Kramer HJM, Amesz J. Thin-layer chromotography of pigments of the green photosynthetic bacterium *Prosthecochloris aestuarii*. Biochim Biophys Acta 1982;681:354–8.
[23] Olson JM, Pedersen JP. Bacteriochlorophyll *c* monomers, dimers, and higher aggregates in dichloromethane, chloroform, and carbon tetrachloride. Photosynth Res 1990;25:25–37.
[24] Dudkowiak A, Francke C, Amesz J. Aggregation of 8,12-diethyl farnesyl bacteriochlorophyll *c* at low temperature. Photosynth Res 1995;46: 427–33.
[25] Dudkowiak A, Francke C, Amesz J, Planner A. Frąckowiak D. Spectral properties of BChl *c* in nematic liquid crystals. II. Aggregated form of dye. Spectrochim Acta A 1996;52:1661–9.
[26] Hansen WN. Reflection spectroscopy of adsorbed layers. Symp Faraday Soc 1970;4:27–35.
[27] Chapados C, Leblanc RM. Aggregation of chlorophylls in monolayers. V. The effect of water on chlorophyll *a* and chlorophyll *b* in mono- and multilayer arrays. Biophys Chem 1983;17:211–44.
[28] Hasegawa T, Umemura J, Takenaka T. Infrared external reflection study of molecular orientation in thin Langmuir–Blodgett films. J Phys Chem 1993;97: 9009–12.
[29] Mielczarski JA, Yoon RH. Fourier transform infrared external reflection study of molecular orientation in spontaneously adsorbed layers on low-absorption substrates. J Phys Chem 1989;93:2034–8.
[30] Ishii T, Uehara K, Ozaki Y, Mimuro M. The effects of pH and ionic strength on the aggregation of bacteriochlorophyll *c* in aqueous organic media: the possibility of two kinds of aggregates. Photochem Photobiol 1999;70:760–5.
[31] Smith KM, Kehres LA, Fajer J. Aggregation of the bacteriochlorophyls *c*, *d* and *e*. Models for the antenna chlorophylls of green and brown photosynthetic bacteria. J Am Chem Soc 1983;105(5):1387–9.
[32] Tamaki H, Holzwarth AR, Schaffner K. Dimerization of synthetic zinc aminochlorins in non-polar organic solvents. Photosynth Res 1994;41:245–51.